molecular pharmaceutics

Article

Cite This: Mol. Pharmaceutics 2019, 16, 3968−3976

pubs.acs.org/molecularpharmaceutics

Distribution of Small Molecular Weight Drugs into the Porcine Lens: Studies on Imaging Mass Spectrometry, Partition Coefficients, and Implications in Ocular Pharmacokinetics

Emma M. Heikkinen,*[,†] Seppo Auriola,[‡] Veli-Pekka Ranta,[†] Nicholas J. Demarais,[§] Angus C. Grey,[∥] Eva M. del Amo,[⊥] Elisa Toropainen,[†,#] Kati-Sisko Vellonen,[†] Arto Urtti,[†,¶,▽] and Marika Ruponen[†]

[†]School of Pharmacy, Biopharmacy Department, [‡]School of Pharmacy, Pharmaceutical Chemistry Department, and [#]Institute of Clinical Medicine, University of Eastern Finland, Yliopistonranta 1, Kuopio 70211, Finland

[§]School of Biological Sciences, University of Auckland, Private Bag 92019, Auckland 1142, New Zealand

[∥]University of Auckland, School of Medical Sciences, Department of Physiology, Private Bag 92019, Auckland 1142, New Zealand

[⊥]School of Health Sciences, Division of Pharmacy & Optometry, University of Manchester, Oxford Road, Manchester M13 9PL, U.K.

[¶]Faculty of Pharmacy, Division of Pharmaceutical Biosciences, University of Helsinki, Viikinkaari, Helsinki 00014, Finland

[▽]Institute of Chemistry, Saint Petersburg State University, 26 Universitetskii Prospect, Saint Petersburg 198504, Russia

Supporting Information

ABSTRACT: Lens is the avascular tissue in the eye between the aqueous humor and vitreous. Drug binding to the lens might affect ocular pharmacokinetics, and the binding may also have a pharmacological role in drug-induced cataract and cataract treatment. Drug distribution in the lens has been studied in vitro with many compounds; however, the experimental methods vary, no detailed information on distribution between the lens sublayers exist, and the partition coefficients are reported rarely. Therefore, our objectives were to clarify drug localization in the lens layers and establish partition coefficients for a wide range of molecules. Furthermore, we aimed to illustrate the effect of lenticular drug binding on overall ocular drug pharmacokinetics. We studied the distribution of 16 drugs and three fluorescent dyes in whole porcine lenses in vitro with imaging mass spectrometry and fluorescence microscopy techniques. Furthermore, we determined lens/buffer partition coefficients with the same experimental setup for 28 drugs with mass spectrometry. Finally, the effect of lenticular binding of drugs on aqueous humor drug exposure was explored with pharmacokinetic simulations. After 4 h, the drugs and the dyes distributed only to the outermost lens layers (capsule and cortex). The lens/buffer partition coefficients for the drugs were low, ranging from 0.05 to 0.8. On the basis of the pharmacokinetic simulations, a high lens-aqueous humor partition coefficient increases drug exposure in the lens but does not significantly alter the pharmacokinetics in the aqueous humor. To conclude, the lens seems to act mainly as a physical barrier for drug distribution in the eye, and drug binding to the lens affects mainly the drug pharmacokinetics in the lens.

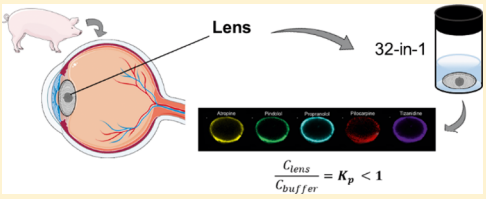

KEYWORDS: *lens, drug distribution, ocular, pharmacokinetics, imaging mass spectrometry, MALDI-IMS*

1. INTRODUCTION

Lens is a transparent, avascular organ positioned in the eye between the aqueous humor and vitreous. The main function of the lens is to change the focal distance of the eye, which ensures the formation of a clear image to the retina with various object distances. The lens consists of the lens capsule, lens anterior epithelial cell monolayer, and lens fiber cells[1] (Figure S1). The lens capsule surrounds the epithelial and fiber cells of the lens and allows the permeation of even large molecules to the lens.[2−4] The lens epithelial cell layer lies in the anterior lens and possesses tight junctions.[5] The fiber cells, named for their long length, are differentiated epithelial cells that have migrated from the anterior lens to the lens equator and further toward the lens center during lens growth. The lens fiber cells can be further divided into loosely structured lens cortex, which consists of the young lens fiber cells, and dense lens nucleus, which consists of the oldest. The main components of the lens are water and proteins, mainly various crystallins, and their concentrations vary between the lens cortex and nucleus, the cortex having higher water and lower protein content than the nucleus.[1] The lens lipids contain a high level of cholesterol, and they are mostly associated with proteins in the cell membranes.[6] Thus, the lipid content of lens also increases from the cortex to the nucleus. For a more

Received: May 28, 2019
Revised: July 19, 2019
Accepted: July 26, 2019
Published: July 26, 2019

DOI: 10.1021/acs.molpharmaceut.9b00585
Mol. Pharmaceutics 2019, 16, 3968−3976

detailed, yet introductory, description of the anatomy of the lens, see the Supporting Information.

The role of lens in ocular pharmacology is known to some extent. First, the lens acts as a physical barrier that limits drug entrance from the anterior chamber to the vitreous and vice versa.[7] Therefore, drug distribution between the anterior and posterior parts of the eye becomes easier in aphakic eyes.[8,9] Second, drugs may bind to the lens, thereby affecting ocular pharmacokinetics. Third, the lens is the target tissue in potential drug treatments of cataract (i.e., lens opacity).[10−12] For a pharmacological effect, the drug must diffuse deep enough into the lens. Studies on anticataract drugs have not explored the actual drug distribution or binding in the lens, though the pharmacological effect indicates that at least a low drug concentration in the target site is achieved. On the other hand, drug binding to the lens may also result in cataract formation, for example, with the use of corticosteroids, phenothiazines, and busulfan.[13]

Drug distribution to the isolated lenses has been studied with various compounds, such as pilocarpine,[14] chloramphenicol,[15] dexamethasone,[15] epinephrine,[15] pilocarpine,[15] timolol,[16] and some aldose reductase inhibitors.[17] Drug distribution between the lens capsule, cortex, and nucleus, however, has not been reported in detail in the literature. One comprehensive study with 13 small molecular weight drugs investigated the in vitro drug partitioning to rabbit lens and linked compound lipophilicity with increased lens-incubate concentration ratio and uptake rate to the lens.[18] This study also reported concentrations of some drugs in the lens capsule and body (lens epithelium and fiber cells) and concluded that lipophilic drugs can penetrate to the lens body and show higher lens affinity than more polar compounds. In these studies, the experimental methods vary, and only rarely actual lens/buffer partition coefficients were reported.

Drug distribution between the lens capsule and the epithelium−cortex−nucleus has been previously studied with radiolabeled compounds, necessitating the mechanical isolation of different layers of the lens.[14] Imaging mass spectrometry (IMS) is a novel technique that should enable analysis of various compounds simultaneously in the lens tissue at high spatial resolution (≈10 μm).[19−21]

In the present work, we aimed to study the localization of various compounds in porcine lens with matrix-assisted laser desorption/ionization IMS (MALDI-IMS) and fluorescence microscopy. Furthermore, we determined the lens/buffer partition coefficients (K_p) for 28 drugs in the isolated porcine lens with liquid chromatography−mass spectrometry (LC−MS/MS). Finally, we illustrated the pharmacokinetic role of lenticular drug distribution with pharmacokinetic simulations.

2. MATERIALS AND METHODS

2.1. Tissue Isolation. Enucleated porcine eyes were received from a local slaughterhouse and transported to the laboratory in cooled 25 mM phosphate-buffered saline (PBS) within 6 h after enucleation. Extraocular tissues were removed from the isolated eyeballs. Then, the eye was cut open from limbus and the lens was collected carefully with a spatula. The lenses were weighed and immediately used in the experiments.

2.2. Extent of Drug Distribution into the Isolated Porcine Lens. *2.2.1. Preparation of the Cassette Mix.* Drug distribution to the lenses was determined by using a mixture of 32 compounds: the compounds and their chemical descriptors, vendors, and solvents for stock solutions are listed in ref.[22] Lornoxicam was excluded from the mix. Stock solutions [0.5−10 mg/mL in PBS or dimethyl sulfoxide (DMSO)] were combined and diluted further with Hanks' balanced salt solution (HBSS)−HEPES (25 mM) (pH 7.4). Octanol−water distribution coefficients of the compounds (log $D_{7.4}$) and polar surface areas (PSAs) were previously estimated in silico from compound structures with ACD/Labs-software (v12, Advanced Chemistry Development, Inc., Canada).[22]

2.2.2. Drug Distribution into the Lens: Studies for MALDI-IMS. 2.2.2.1. Incubation. To determine distribution of cassette mix drugs in the lens, the isolated porcine lenses (n = 10) were incubated in 1200 μL of prewarmed drug solution in capped flat-bottomed polystyrene vials sealed with parafilm at +35 °C in a horizontal shaker (Heidolph incubator 1000, Heidolph Elektro GmbH & Co., Germany) at 150 rpm shaking. After 4 h, the buffer was removed from the vials and the lenses were rinsed with HBSS−HEPES and gently blotted dry. The lenses were weighed, snap-frozen with liquid nitrogen in flat-bottomed plastic tubes, and then stored at −80 °C until sample preparation and analysis with MALDI-IMS. For the experiment, a smaller set of 16 drugs was used. The final incubation mixture of drugs consisted of acetazolamide, ampicillin, atenolol, atropine, betaxolol, carteolol, ciprofloxacin, ketorolac, lincomycin, nadolol, pilocarpine, pindolol, and propranolol, each at 10 μg/mL. Also, aztreonam, methazolamide, and tizanidine were included at 100 μg/mL. Final DMSO concentration of the solution was 2%.

2.2.2.2. Tissue Preparation. The frozen lenses were mounted onto a chuck using an optimal cutting temperature compound (Sakura Finetek, CA, USA) on the equatorial side. The lenses were sectioned to 10 μm thickness at −20 °C on a Leica CM Cryostat (S3050, Leica Microsystems GmbH, Germany), equipped with a FEATHER Microtome C35 blade (pfm medical, UK), and collected on a cryofilm (3C16UF, SECTION-LAB Co. Ltd. Yokohama, Japan) by modified Kawamoto method.[23] The film was subsequently mounted onto a microscopy glass slide using a double-sided copper tape. The slides were washed twice with 50 mM ammonium formate for 30 s and dried in a vacuum desiccator. The sample slides contained three lens sections from the drug mixture experiment and three blanks. To quantify the amount of each compound present in incubated lenses, 1 μL of standard mixture was added on one of the blank lenses using concentrations of 0.1, 0.5, 2, and 10 μg/mL. First, the internal standard solution of atropine-d_5 (200 ng/mL in 50% acetonitrile) was sprayed to obtain a 10.2 ng/cm^2 corresponding to approximately 10 μg/g in the tissue. Matrix α-cyano-4-hydroxycinnamic acid (7 mg/mL in 50% acetonitrile containing 1% trifluoro acetic acid) (Sigma-Aldrich, St. Louis, MO, USA) was added via spray deposition using 10 passes, flow rate of 100 μL/min, temperature of 77 °C, track spacing of 2.5 mm, and velocity of 1300 mm/min (HTX Industries, TM-Sprayer, NC, USA).

2.2.2.3. Fourier Transform-Ion Cyclotron Resonance-IMS. MALDI Fourier transform-ion cyclotron resonance (FT-ICR)-IMS was performed using a Bruker 7T solariX XR mass spectrometer (Bruker Daltonics, Germany) at a 75 μm spatial resolution. Spectra were collected in positive ion mode in mass-to-charge ratio (m/z) range of 100−1000, and the resolution was 61 000 at m/z 307. The compounds and m/z values ($[M + H]^+$) used were as follows: atropine 290.1751, propranolol 260.1645, atenolol 267.1703, carteolol 293.18601860, pilocarpine 209.1285, methazolamide

DOI: 10.1021/acs.molpharmaceut.9b00585
Mol. Pharmaceutics 2019, 16, 3968−3976

237.0111, pindolol 249.1598, tizanidine 254.0262, nadolol 310.2013, lincomycin 407.2210, and fluconazole 307.1113.

2.2.2.4. Analysis of FT-ICR Data and Image Processing. FT-ICR data were read into Fleximaging 4.1 software (Bruker Daltonics, Germany) and normalized against the d_5-atropine internal standard signal at m/z 295. The drugs were identified as their $[M + H]^+$ ions. Peak finding was performed using mass error less than 2.5 ppm. MALDI images for each detected compound were plotted using a 0.01 μ mass window. From the images of the individual drugs, the intensity profiles across a 30 pixel (2.25 mm) wide area in anterior−posterior axis were plotted with ImageJ software (National Institutes of Health, USA).

2.2.3. Partition Coefficients for Cassette Mix Drugs. 2.2.3.1. Incubation. To determine the K_p values, the distribution study was conducted as described in Section 2.2.2, but the incubation volume (300 μL), the number of drugs, and the drug concentrations in the cassette mix were different. For this experiment, the whole mix of 32 drugs was used. The test concentrations of the drugs in the cassette mix were 1 and 10 μg/mL: 1 μg/mL was used for all compounds except aztreonam, bromfenac, dexamethasone, diclofenac, fluorometholone, indomethacin, levocabastine, methazolamide, prednisolone, quinidine, and tizanidine. For these compounds, a concentration of 10 μg/mL was used. Two different drug concentrations were used to ensure reliable quantitation in the LC−MS/MS analyses. The DMSO concentration of the final mixture was 0.9%. The lenses were stored at −80 °C until sample preparation and analysis with LC−MS/MS.

2.2.3.2. Sample Preparation for LC−MS/MS. The lenses were homogenized first with plastic homogenization pestles and then with ULTRA-TURRAX (model T8, IKA-Werke GmbH & Co. KG, Germany) in HBSS−HEPES (1 g lens + 9 mL buffer). Lens homogenate (200 μL) was mixed with 400 μL of methanol (Chromasolv LC−MS Ultra, Honeywell Riedel-de Haën, NC, USA), containing internal standards atenolol-d_7 (Toronto Research Chemicals Inc., Canada), atropine-d_5 (Toronto Research Chemicals Inc., Canada), fluconazole-d_4 (Toronto Research Chemicals Inc., Canada), and lincomycin-d_3 (Toronto Research Chemicals Inc., Canada) at 24.4 ng/mL each and vortexed. The samples were centrifuged at 16 060g for 10 min at +4 °C and their supernatants were collected and stored at −20 °C. On the day of LC−MS run, the sample supernatants (300 μL) were filtered through a Captiva ND lipid-plate (Agilent Technologies, CA, USA) to a Captiva 96 deep well collection plate (Agilent Technologies, CA, USA) by centrifugation at 1560g for 40 min at +4 °C. Duplicate standards (eight levels, 5−1000 ng/mL) and triplicate quality control (QC) samples (50, 250 and 1000 ng/mL) were prepared from cassette mix working solutions in a similarly diluted lens homogenates as the actual samples.

2.2.3.3. LC−MS/MS Analysis. For detailed description of the LC−MS/MS acquisition method, see ref 22. For the LC−MS/MS analyses, the lens samples were run in two separate analysis batches with independent standards and QC samples. The resulting data were analyzed with Agilent MassHunter Quantitative Analysis software (vB.09.00, build 9.0.647.0, Agilent Technologies, CA, USA). Internal standards were used in the calculations. The calibration curves were calculated from duplicate standard series, one of which was run in the beginning and the other at the end of each analysis. Quadratic fitting with $1/x$ weighing was used. The criteria for calibration curve and QC acceptance were 80−120% accuracy of mean for ≥66.7% of calibration levels and at LLOQ, 80−120% accuracy for ≥66.7% of individual QCs and QC levels and <20% coefficient of variation for ≥66.7% of QC levels. The selectivity criterion of ≥3-fold response ratio of LLOQ to matrix-based blank sample was employed.

2.2.3.4. Calculation of Lens/Buffer Partition Coefficients (K_p). From the LC−MS/MS results, K_p values were first calculated using the total lens volume (eq 1)

$$K_p = \frac{C_{lens,4h}}{C_{inc,4h}} = \frac{m_{lens,4h}/V_{lens}}{C_{inc,init} - m_{lens,4h}/V_{inc}} \quad (1)$$

where $C_{lens,4h}$ is the drug concentration in the lens at 4 h (ng/mL), $C_{inc,4h}$ is the drug concentration in the incubate at 4 h (ng/mL), $m_{lens,4h}$ is the drug amount in the lens at 4 h (ng), V_{lens} is the lens volume (mL) (calculated with the actual lens mass and lens density of 1.183 g/mL[24]), $C_{inc,init}$ is the initial drug concentration in the incubate (ng/mL), and V_{inc} is the volume of the buffer (mL).

The drug concentration in the incubate at 4 h was calculated by using the initial drug concentration in the buffer ($C_{inc,init}$), buffer volume (V_{inc}), and drug amount in the lens at 4 h ($m_{lens,4h}$) instead of the measured concentration in the incubate because the concentration in the incubate showed very little decrease (<5−10%) during the incubation. K_p values were also calculated with the actual lens volume into which the compounds distribute based on the MALDI IMS data (true distribution volume instead of the total lens volume) (see the Supporting Information). The same approximation for the volume of distribution was assumed for all cassette mix compounds.

2.3. Distribution Patterns of Fluorescent Dyes within the Lens. *2.3.1. Fluorescent Dyes.* The distribution patterns of the compounds in the porcine lenses were studied with three fluorescent dyes with varying lipophilicities. Rhodamine-B and fluorescein sodium (Sigma-Aldrich) were dissolved into HBSS−HEPES (pH 7.4) at 1 mg/mL concentration. Rhodamine-123 (Sigma-Aldrich) was first dissolved into ethanol (10 mg/mL) and then diluted in HBSS−HEPES (pH 7.4) to reach 0.1 mg/mL (final ethanol concentration was 1%).

2.3.2. Incubation. The distribution studies with fluorescent dyes were conducted separately for each dye, as described in Section 2.2.2, with an incubation volume of 1200 μL. After incubation, the lenses were rinsed, blotted dry, frozen in an optimal cutting temperature compound (Sakura Finetek, SA, USA) in plastic tubes with chilled 2-propanol, and stored at −20 °C until cryosectioning.

2.3.3. Fluorescence Microscopy. The lenses were sectioned to a thickness of 10 μm at −20 °C with Leica CM cryostat (Leica 3050S, Leica Microsystems GmbH, Germany) equipped with a FEATHER Microtome C35 blade (pfm medical, UK) and collected on a SuperFrost Plus adhesion microscope slide (Thermo Fisher Scientific, MA, USA). The tissue slices were imaged with a fluorescence microscope (Zeiss Axio Imager M2, Carl Zeiss Microscopy GmbH, Germany) equipped with filters 470 nm (65HEAF488) and 590 nm (64HEmPlum) filters and Axiocam MRm camera (Carl Zeiss Microscopy GmbH, Germany) using a 2.5-fold magnification. Exposure times were 600 ms for fluorescein sodium, 600 ms for rhodamine-B, and 1 s for rhodamine-123. Individual images of the lens sections were merged together manually with GNU image processing software (v2.10.6).

DOI: 10.1021/acs.molpharmaceut.9b00585
Mol. Pharmaceutics 2019, 16, 3968−3976

2.4. Pharmacokinetic Simulations. *2.4.1. Model Structure and Parameters.* A pharmacokinetic simulation model for rabbit was built for topical timolol instillation based on the model of Ranta et al.[25] The lens compartment, separate from the reservoir compartment, was added to the model (Figure 1).

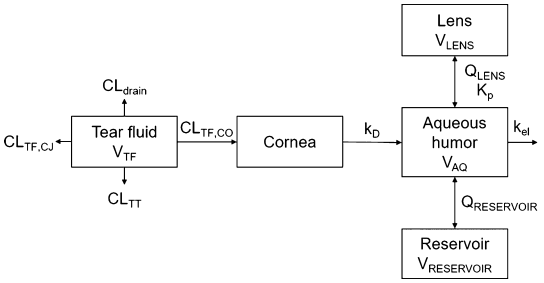

Figure 1. Simulation model for timolol distribution to the lens after topical dosing, extended from ref 25. V_{TF}, tear fluid volume; $CL_{TF,CJ}$, clearance from tear fluid by conjunctival absorption; CL_{TT}, clearance from tear fluid by tear turnover; CL_{drain}, clearance from tear fluid by drainage of the instilled solution; $CL_{TF,CO}$, clearance from tear fluid by corneal absorption; k_D, corneal desorption rate constant; V_{AQ}, aqueous humor volume; k_{el}, elimination rate constant; $Q_{RESERVOIR}$, distribution clearance between aqueous humor and reservoir; $V_{RESERVOIR}$, reservoir volume; K_p, lens/buffer partition coefficient; Q_{LENS}, distribution clearance between aqueous humor and the lens; V_{LENS}, lens volume.

The unknown parameter values for timolol distribution clearance between aqueous humor and lens (Q_{LENS}), K_p, and clearance from tear fluid to cornea ($CL_{TF,CO}$) were obtained by adjusting the values manually until the simulated concentration in the lens matched with in vivo data on timolol distribution to the rabbit lens.[26] Finally, the distribution clearance between the aqueous humor and the reservoir ($Q_{RESERVOIR}$) and the volume of the reservoir ($V_{RESERVOIR}$) were adjusted to match the corresponding parameters in the original model. For details of the model building and parameters, see the Supporting Information. STELLA software (v8.1.1, isee systems) was used to construct the simulation model.

2.4.2. Simulations. Kinetic simulations were carried out to estimate how drug partitioning into the lens might affect ocular pharmacokinetics after single and multiple doses of eye drops. In the simulations, a single and repeated dosing (every 24 and 8 h) of 125 μg of timolol (0.5%, 25 μL) were used. The run time was 7 days and the delta time was 0.5 min. Simulations were run with K_p values of 0.35, 1.05 (3-fold increase), and 3.5 (10-fold increase) to see the potential impact of lens partitioning on ocular pharmacokinetics.

3. RESULTS

3.1. Lens Integrity. The lens should retain its integrity during the incubation with drugs. Therefore, the integrity was evaluated by monitoring the lens mass (Figure S2) and appearance at different times. During 4 h of incubation, the mass was retained at 469 ± 55.8 mg, and no change in the lens mass was observed. Furthermore, the lenses did not show damage or swelling during the experiments. However, in a preliminary experiment, a clear decrease in the lens mass was seen at longer incubation times. The remaining mass, compared to the original, was 81.3 ± 11.0% (n = 2) at 12 h and 67.2 ± 16.8% (n = 10) at 24 h of incubation (Figure S2). Furthermore, after 4 h, the lens capsule and cortex began swelling and came off by 12 h. For this reason, longer incubations were not feasible and incubations of 4 h were used in the experiments.

3.2. Drug and Dye Distribution Patterns in the Lens. The distribution patterns of the cassette mix drugs in the porcine lens were evaluated using MALDI-IMS. Eleven (atenolol, atropine, carteolol, fluconazole, lincomycin, methazolamide, nadolol, pilocarpine, pindolol, propranolol, and tizanidine) out of the 16 compounds gave acceptable signals when standard solution was loaded on a blank lens section (Figure S3). When the drug amount in the pipetted standard solutions exceeded 2 ng per spot, the internal standard atropine-d_5 signal was suppressed (Figure S4).

In the lens samples, atropine, pilocarpine, pindolol, propranolol, and tizanidine (in silico predicted log $D_{7.4}$ range from −1.09 to 2.04) showed distribution only in the capsule and cortex of the lens but not in the nucleus (Figure 2). The posterior rim showed 1.2- to 2-fold higher intensities than the anterior rim (Figure 3). In general, the signal intensity–distance profiles for the drugs were similar. For aztreonam, lincomycin, methazolamide, and nadolol, the signals at their m/z were detected in the drug-incubated lens sample, but also in the blank lenses. This indicates that the signals originated from some endogenous compounds with the same m/z within our experimental error. These compounds were therefore excluded from further analysis. In the average spectrum taken from the lens posterior surface (thickness 1 mm), the intensity measured for d_5-atropine was 850 and for atropine 290 (Figure

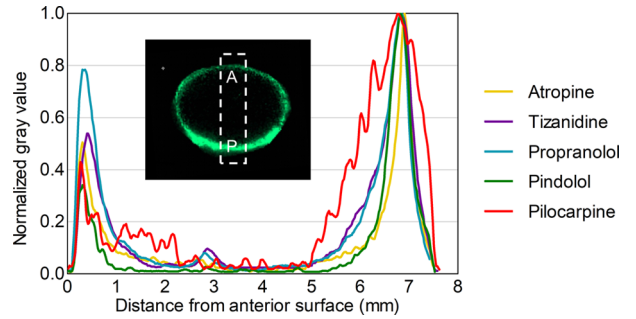

Figure 3. Relative drug distribution along the anterior–posterior axis in a porcine lens after 4 h in vitro incubation.

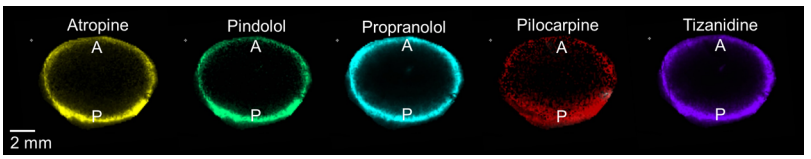

Figure 2. Drug distribution in a porcine lens after 4 h in vitro incubation. m/z signals across a lens section were obtained with MALDI-IMS and normalized to internal standard atropine-d_5 signal. A = anterior lens pole, P = posterior lens pole.

DOI: 10.1021/acs.molpharmaceut.9b00585
Mol. Pharmaceutics 2019, 16, 3968–3976

S5). On the basis of the ratio, the concentration of atropine is estimated to be 3.4 μg/g.

Distribution studies were also performed with fluorescent dyes with different lipophilicities. The dyes did not penetrate into the lens nucleus in 4 h and, thus, fluorescence imaging data were in accordance with the MALDI-IMS results. Rhodamine-B (experimental log $D_{7.0}$ = 2[27]) distributed slightly deeper into the lens cortex than rhodamine-123 (experimental log $D_{7.0}$ = 0.4[28]) and fluorescein sodium (experimental log $D_{7.0}$ = 0.1[29]) (Figure 4).

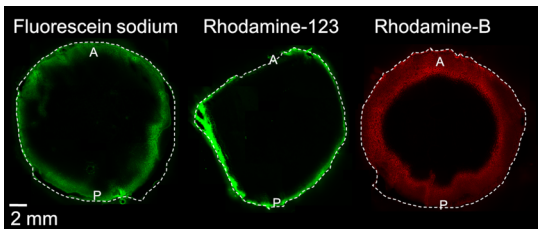

Figure 4. Distribution of fluorescein (log $D_{7.0}$ = 0.1), rhodamine-123 (log $D_{7.0}$ = 0.4), and rhodamine-B (log $D_{7.0}$ = 2) into the porcine lens in vitro after 4 h incubation. A = anterior lens, P = posterior lens.

3.3. Lens/Buffer Partition Coefficients. Lens/buffer K_p values were obtained for 28 out of 32 drugs by analyzing the drug amounts in whole porcine lenses with LC−MS/MS. The whole lens volume was used in the calculations (eq 1). The K_p values were <1.0 for all compounds and <0.5 for most of them (Figure 5). The range was from 0.047 (methazolamide) to 0.762 (propranolol).

The apparent volume of drug distribution was estimated from the MALDI-IMS data. On the basis of the MALDI-IMS images of atropine, pindolol, propranolol, pilocarpine, and tizanidine, the five drugs had a similar spatial distribution despite having different log $D_{7.4}$ values, and we estimated that the drugs distributed to 27.1% of the total lens volume (see the Supporting Information and Equation S1). This volume was used for all cassette mix compounds. The use of this volume in the calculations resulted in higher K_p values (Figure 5), ranging from 0.172 (methazolamide) to 2.810 (propranolol). Still, only six compounds (propranolol, quinidine, voriconazole, betaxolol, tizanidine, and diclofenac) had K_p > 1.

The K_p values did not show correlation with in silico-predicted log $D_{7.4}$ within the entire group of drugs (Figure 6, panel A), even though the highest K_p values were seen for compounds with log $D_{7.4}$ > 0. Furthermore, the series of β-blockers nadolol, atenolol, carteolol, pindolol, betaxolol, and propranolol showed increasing K_p with increasing log $D_{7.4}$ (Figure 6, panel A). PSA showed an inverse correlation with K_p in the whole group of drugs (Figure 6, panel B).

We did not obtain K_p values for acyclovir, ganciclovir, aztreonam, and fluorometholone because their quantitative analyses did not meet the acceptance criteria.

3.4. Pharmacokinetic Simulations. Pharmacokinetic simulations of a single topical timolol eye drop were carried out with three lens/buffer K_p values (0.35, 1.05, and 3.5) to see, whether drug partitioning to the lens affects drug concentrations or area under the curve (AUC) values in the aqueous humor and the lens. The simulations were also run with repeated dosing of eye drops at 8 and 24 h intervals.

3.4.1. Single Topical Dose. Neither the simulated peak concentration nor the shape of the concentration−time curve in aqueous humor were notably affected by the lens K_p (Table 1; Figure 7, panel A). In the lens, the peak concentration with K_p of 0.35 was 0.28 μg/mL, and with K_p values of 1.05 and 3.5, it was 1.3- and 1.5-fold higher, respectively (Table 1; Figure 7, panel B). Also, AUC_{0-14d} in the lens increased from 111 μg·min/mL 3- and 10-fold, when K_p was increased from 0.35 to 1.05 and 3.5, respectively. At 8 h, the drug concentration in aqueous humor was close to 0 regardless of the K_p values, whereas in the lens, the concentration was >0.1 μg/mL with all K_p values. The drug concentration in the lens remained above 0 for roughly 1, 2, and 8 days with K_p values of 0.35, 1.05, and 3.5, respectively.

3.4.2. Repeated Dosing. With every 24 h dosing, the peak concentration in aqueous humor did not change considerably with increasing K_p values (Table 1; Figure 8, panel A). Between the doses, the concentration in aqueous humor dropped to zero with all K_p values. In the lens, the peak concentration at steady state was 0.28 μg/mL with K_p of 0.35, and it increased to 1.5- and 3.4-fold with K_p values of 1.05 and 3.5, respectively (Table 1; Figure 8, panel B). With the lowest K_p (0.35), the concentration in the lens reached 0 between the doses, whereas with K_p values of 1.05 and 3.5, the minimum concentrations at steady state were 0.08 and 0.58 μg/mL, respectively.

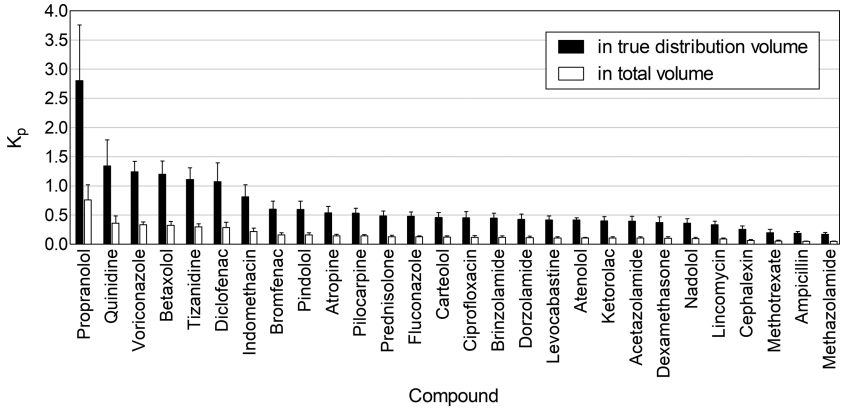

Figure 5. In vitro lens/buffer partition coefficients (K_p) for the drugs after 4 h incubation with the porcine lens. The K_p values were calculated based on the imaged volume of distribution and total anatomical volume of the lens. Mean ± standard deviation (SD), n = 10, except for atenolol n = 5.

DOI: 10.1021/acs.molpharmaceut.9b00585
Mol. Pharmaceutics 2019, 16, 3968−3976

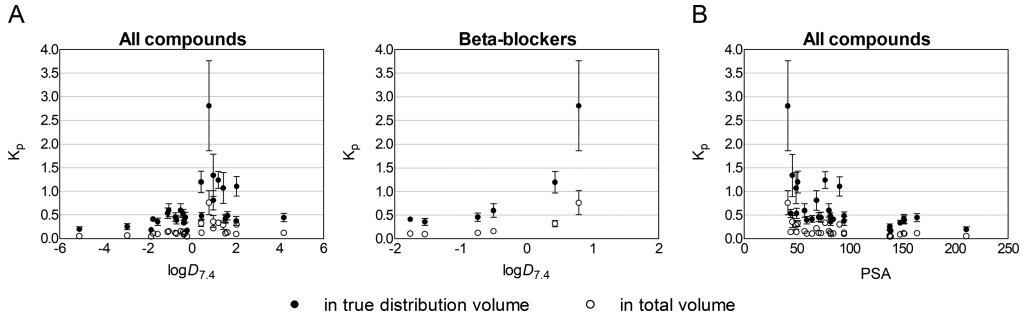

Figure 6. Relationship between in vitro lens/buffer partition coefficient (K_p) (mean ± SD, n = 5−10) and compound lipophilicity (log $D_{7.4}$ and PSA) for all of the studied compounds and a series of β-blockers nadolol, atenolol, carteolol, pindolol, betaxolol, and propranolol. The K_p values were calculated by using both the image-based distribution volume and the total anatomical volume of the lens.

Table 1. Simulated Timolol Concentrations and AUCs in the Aqueous Humor and Lens with Various Lens/Buffer Partition Coefficients (K_p) and Dosing Schemes

			K_p		
			0.35	1.05	3.5
single dose of 125 μg (25 μL)	aqueous humor	C_{max} (μg/mL)	2.79	2.79	2.79
		$AUC_{0-14days}$ (μg·min/mL)	318	318	318
	lens	C_{max} (μg/mL)	0.28	0.36	0.42
		$AUC_{0-14days}$ (μg·min/mL)	111	333	1111
125 μg (25 μL) once daily	aqueous humor	$C_{max,ss}$ (μg/mL)	2.79	2.79	2.80
		$C_{min,ss}$ (μg/mL)	0.00	0.00	0.00
	lens	$C_{max,ss}$ (μg/mL)	0.28	0.43	0.95
		$C_{min,ss}$ (μg/mL)	0.00	0.08	0.58
125 μg (25 μL) three times daily	aqueous humor	$C_{max,ss}$ (μg/mL)	2.80	2.81	2.81
		$C_{min,ss}$ (μg/mL)	0.01	0.02	0.02
	lens	$C_{max,ss}$ (μg/mL)	0.34	0.80	2.42
		$C_{min,ss}$ (μg/mL)	0.11	0.55	2.16

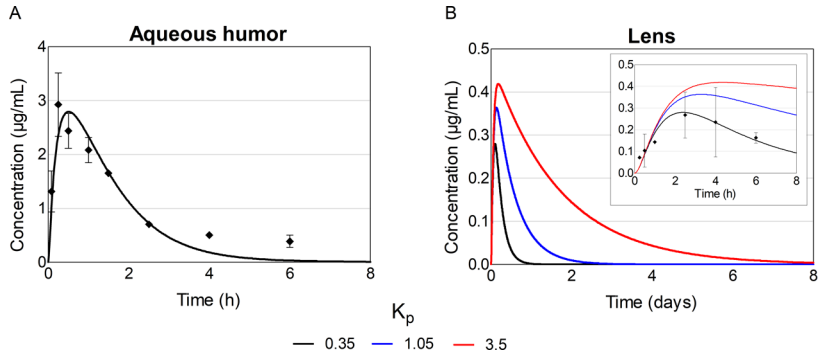

Figure 7. Simulated timolol concentrations in the aqueous humor and lens after a single 125 μg topical dose to rabbit with different lens/buffer partition coefficient (K_p) values. The dots present observed timolol concentrations in vivo[26] while the lines present the simulated ones. For aqueous humor, the lines with various K_p values overlap each other.

With every 8 h dosing, neither the peak nor the minimum concentration in aqueous humor changed markedly with increasing K_p (Table 1; Figure 8, panel C). In the lens, the peak concentrations at steady state increased from 0.34 μg/mL (K_p 0.35) to 2- and 7-fold with K_p values of 1.05 and 3.5, respectively (Table 1; Figure 8, panel D). With a K_p of 0.35, the minimum concentration at steady state was 0.11 μg/mL, and it increased 5- and 20-fold with K_p values of 1.05 and 3.5, respectively.

4. DISCUSSION

Drug binding to the lens has a role in ocular pharmacokinetics, pharmacology, and drug delivery. To our knowledge, this is the first study that explores lenticular drug distribution using a wide range of drugs and dyes. We showed that the extent of drug distribution to the porcine lens during 4 h in vitro incubation is low regardless of the compound properties. The K_p values of all drugs ranged from 0.05 to 0.8. Furthermore, the pharmacokinetic simulations indicated that drug partitioning to the lens does not affect drug concentrations in the aqueous humor but increases the AUC and drug concen-

DOI: 10.1021/acs.molpharmaceut.9b00585
Mol. Pharmaceutics 2019, 16, 3968−3976

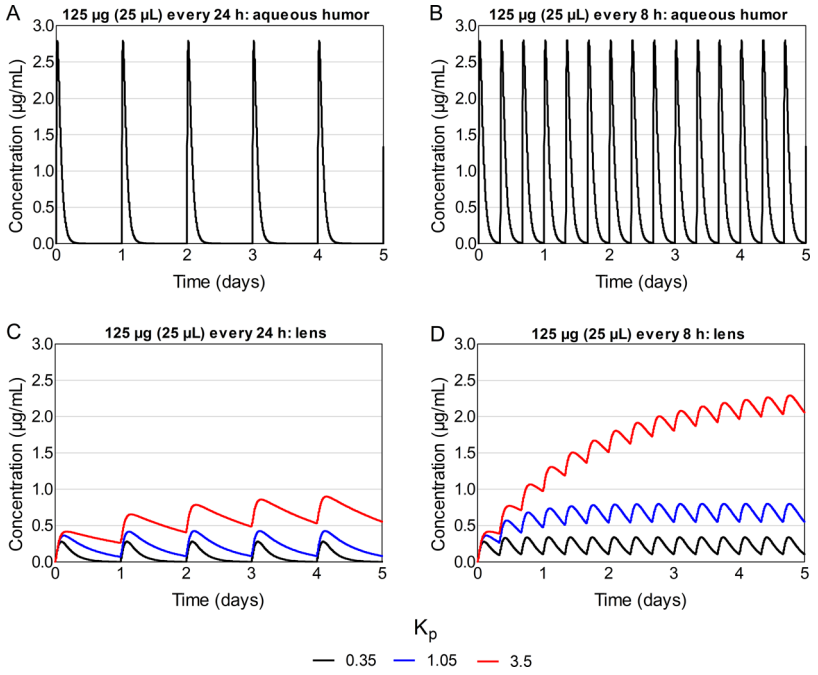

Figure 8. Simulated timolol concentrations in the aqueous humor and lens after repeated topical dosing with different lens/buffer partition coefficients (K_p). For aqueous humor, the lines with various K_p values overlap each other.

trations in the lens. It seems that drug partitioning to the lens has pharmacological significance only if the site of drug action or toxicity is in the lens.

Lens partition coefficients with a broad set of compounds using the same method have not been presented previously. In general, the K_p values in previous reports have ranged from about 0.3 (pilocarpine[15]) to 8 (aldose reductase inhibitor CT-112[17]). The results of this study are roughly in line with previously published or recalculated in vitro K_p values. As examples from previous literature, pilocarpine has a K_p of 0.3−1.0 in rabbit[14] and human[15] and dexamethasone 0.3−0.5 in human.[15] Our K_p values for pilocarpine (0.145) and dexamethasone (0.102) are slightly lower, but in the same range as the previous data. Small differences may be caused by test conditions (e.g., incubation time) and species differences in lens biochemistry (e.g., protein content[11]). Tang-Liu et al.[18] reported higher lens/buffer K_p values, more than 5, for lipophilic compounds, but they used a long incubation time of 24 h. In our experience, longer than 4 h incubation times resulted in the loss of lens integrity that may lead to overestimation of drug distribution into the lens.

For most compounds, the incubation time of 4 h was long enough to reach the concentration equilibrium between the incubate and the lens (see Figure S7). Some compounds such as ciprofloxacin and diclofenac would have required longer incubation time to reach true equilibria, which might lead to underestimation of their K_p values. However, it is evident that drug distribution to the lens differs substantially from drug distribution into the iris and ciliary body. The low K_p values for the lens are in line with ocular pharmacokinetics in vivo, as concentrations of several drugs (timolol, pilocarpine, atropine, and dexamethasone) in the lens in vivo are much lower than in the aqueous humor, iris, and ciliary body.[14,19,26,30,31] Low K_p values are also in line with a report by del Amo et al.,[32] which demonstrated that the ocular volume of distribution of intravitreally injected 40 small and 12 macromolecular drugs was within a narrow range, close to the anatomical volume of the vitreous.

Interestingly, the drugs and dyes consistently distributed only to the capsule, epithelium, and cortex of the lens, but not to the lens nucleus. Similar findings have been reported for radiolabeled timolol in vivo[33] and arginine vasopressin and progesterone in vitro.[18] The distribution pattern may be explained by the weaker barrier properties in the lens capsule and cortex as compared to the lens nucleus. The lens capsule allows even permeation of macromolecules, such as dextrans (up to 150−160 kDa),[2,3] and proteins.[4] Thus, it does not hinder the distribution of the small molecular weight drugs to the lens epithelium and cortex. The lens cortex consists of the younger, softer lens fiber cells, whereas the older fiber cells are tightly packed in the lens nucleus. This change in the organization of the lens fibers, higher protein concentration in the nucleus, and the decrease in extracellular space probably hinder the permeation of even lipophilic small molecular weight drugs to the lens nucleus. Overall, the tight proteinaceous structure and low lipid content of the lens seem to result in low K_p values. The K_p values in total tissue volume were <1.0, and even in the case of true distribution volume, the K_p values exceeded 1.0 only in few cases. Relatively low lipid content of the lens may explain the correlation and inverse correlation of K_p with log $D_{7.4}$ and PSA, respectively, at low overall levels of K_p values. In the whole heterogeneous group, the correlation with log $D_{7.4}$ was not clear, even though we used compounds with distinct levels of hydrophilicity and lipophilicity. For example, the log $D_{7.4}$ values spanned from −5.10 (methotrexate) to +4.19 (brinzolamide). Moreover, in the anterior lens, the lens epithelium with tight junctions[33] may slow down drug diffusion to the lens fiber cells. Accordingly, the intensities of MALDI-IMS signals were higher in the posterior than in the anterior lens.

In the pharmacokinetic simulations, drug partitioning to the lens virtually did not affect the drug concentration in the aqueous humor despite repeated dosing and a K_p value of 3.5.

DOI: 10.1021/acs.molpharmaceut.9b00585
Mol. Pharmaceutics 2019, 16, 3968−3976

The reason for this is the relatively slow intercompartmental clearance between the lens and aqueous humor over-run by the faster elimination from the aqueous humor. The partitioning to the lens did however increase the AUC and drug concentrations in the lens substantially even after a single topical dose. The change was especially prominent with repeated dosing. On the basis of the simulations, drug partitioning to the lens affects mainly the drug exposure in the lens, but not in the aqueous humor, and hypothetically also not in the surrounding tissues such as iris, ciliary body, and trabecular meshwork.

To our knowledge, MALDI-IMS has not been used before to analyze drug-like compounds in the ocular lens. With IMS, the relative and absolute quantitation suffers markedly from competition and suppression caused by endogenous compounds, mainly lipids and salts. However, signal intensity normalization and the use of isotope-labeled standards can enhance the quantitation,[34] and at the very least, IMS can generate qualitative data on drug distribution within the tissue. In our MALDI-IMS analysis, increasing concentrations of the drug mix standards caused partial suppression of the internal standard (d_5-atropine) signal. Thus, despite the use of an isotope-labeled standard, no exact quantitative concentrations were obtained. However, it is reasonable to estimate that at low concentrations, the ratio of drug and d_5-atropine reflects the concentration of the drug in the tissue. Thus, we used the relative signal of each drug across the lens section to estimate the distribution patterns. To conclude, the MALDI-IMS is a powerful new tool in lenticular drug distribution studies, and possibly also in other ocular pharmacokinetic investigations. Further work is needed to reach accurate calibration curves and quantitative analyses of the drugs in the lens tissue sections.

To conclude, we have determined the in vitro partition coefficients (K_p) and the distribution patterns of various drugs in the porcine lens. The extent of lenticular distribution drug distribution is low ($K_p < 1$) and the drugs do not distribute to the lens nucleus in 4 h. Furthermore, it seems that the impact of drug distribution to the lens has minimal impact on drug concentrations in the aqueous humor, while lenticular distribution is obviously an important factor for drug if the drug has effects in the lens. It seems that drug concentrations in the aqueous humor are determined by drug absorption to the anterior chamber and its clearance from the aqueous humor (via trabecular meshwork and blood flow of anterior uvea). However, the lens forms a dense barrier between the anterior chamber and the vitreous, thereby limiting drug distribution from the anterior chamber to the vitreous and vice versa.

■ ASSOCIATED CONTENT

Supporting Information

The Supporting Information is available free of charge on the ACS Publications website at DOI: 10.1021/acs.molpharmaceut.9b00585.

Lens structure; location of the lens in the eye and its structure; lens mass during incubation; calibration series for MALDI IMS; atropine-d_5 signal suppression by drug mix; IMS spectrum of posterior lens; calculation of the apparent volume of distribution in the lens; building of the pharmacokinetic simulation model; parameter values for pharmacokinetic model; concentration−time curves in aqueous humor and lens with different K_p values; and drug concentration in the incubate (PDF)

■ AUTHOR INFORMATION

Corresponding Author

*E-mail: emma.heikkinen@uef.fi. Phone: +358442110055.

ORCID

Emma M. Heikkinen: 0000-0001-5923-7289
Nicholas J. Demarais: 0000-0002-0666-9405
Arto Urtti: 0000-0001-6064-3102

Notes

The authors declare no competing financial interest.

■ ACKNOWLEDGMENTS

This work was funded by the Doctoral Programme in Drug Research (University of Eastern Finland), Academy of Finland (grant number 233114), Biocenter Kuopio, Biocenter Finland, and Päivikki and Sakari Sohlberg Foundation. E.M.d.A. was supported by the European Union's Horizon 2020 research and innovation programme under the Marie Sklodowska-Curie (grant no. 799880). The authors acknowledge Lea Pirskanen for the technical assistance in the partitioning studies and sample preparation.

■ ABBREVIATIONS

FT-ICR, Fourier transform-ion cyclotron resonance; K_p, lens/buffer partition coefficient; log $D_{7.0}$, octanol−water distribution coefficient at pH 7.0; log $D_{7.4}$, octanol−water distribution coefficient at pH 7.4; MALDI-IMS, matrix-assisted laser desorption/ionization imaging mass spectrometry; m/z, mass-to-charge ratio; PBS, phosphate-buffered saline; PSA, polar surface area; QC, quality control

■ REFERENCES

(1) Dai, E.; Boulton, M. E. Basic science of the lens. In *Ophthalmology*; Yanoff, M., Diker, J., Eds.; Elsevier: Edinburgh, 2018; pp 381−393.

(2) Kastner, C.; Löbler, M.; Sternberg, K.; et al. Permeability of the anterior lens capsule for large molecules and small drugs. *Curr. Eye Res.* **2013**, *38*, 1057−1063.

(3) Lee, C. J.; Vroom, J. A.; Fishman, H. A.; Bent, S. F. Determination of human lens capsule permeability and its feasibility as a replacement for bruch's membrane. *Biomaterials* **2006**, *27*, 1670−1678.

(4) Danysh, B. P.; Patel, T. P.; Czymmek, K. J.; et al. Characterizing molecular diffusion in the lens capsule. *Matrix Biol.* **2010**, *29*, 228−236.

(5) Unakar, N. J.; Johnson, M. J.; Hynes, K. Permeability studies in neonatal rat lens epithelium. *Lens Eye Toxic. Res.* **1991**, *8*, 75−99.

(6) Borchman, D.; Yappert, M. C. Lipids and the ocular lens. *J. Lipid Res.* **2010**, *51*, 2473−2488.

(7) Maurice, D. M.; Mishima, S. *Ocular Pharmacology*; Springer: Berlin, Heidelberg, 1984; pp 19−116.

(8) Christoforidis, J. B.; Williams, M. M.; Wang, J.; et al. Anatomic and pharmacokinetic properties of intravitreal bevacizumab and ranibizumab after vitrectomy and lensectomy. *Retina* **2013**, *33*, 946−952.

(9) Meredith, T. A.; Aguilar, H. E.; Shaarawy, A.; Kincaid, M.; Dick, J.; Niesman, M. R. Vancomycin levels in the vitreous cavity after intravenous administration. *Am. J. Ophthalmol.* **1995**, *119*, 774−778.

(10) Makley, L. N.; McMenimen, K. A.; DeVree, B. T.; et al. Pharmacological chaperone for α-crystallin partially restores transparency in cataract models. *Science* **2015**, *350*, 674−677.

DOI: 10.1021/acs.molpharmaceut.9b00585
Mol. Pharmaceutics 2019, 16, 3968−3976

(11) Abdelkader, H.; Alany, R. G.; Pierscionek, B. Age-related cataract and drug therapy: Opportunities and challenges for topical antioxidant delivery to the lens. *J. Pharm. Pharmacol.* **2015**, *67*, 537−550.
(12) Thrimawithana, T. R.; Rupenthal, I. D.; Räsch, S. S.; Lim, J. C.; Morton, J. D.; Bunt, C. R. Drug delivery to the lens for the management of cataracts. *Adv. Drug Delivery Rev.* **2018**, *126*, 185−194.
(13) Li, J.; Tripathi, R. C.; Tripathi, B. J. Drug-induced ocular disorders. *Drug Saf.* **2008**, *31*, 127−141.
(14) Miller, S. C.; Himmelstein, K. J.; Patton, T. F. A physiologically based pharmacokinetic model for the intraocular distribution of pilocarpine in rabbits. *J. Pharmacokinet. Biopharm.* **1981**, *9*, 653−677.
(15) Heyrman, T. P.; McDermott, M. L.; Ubels, J. L.; Edelhauser, H. F. Drug uptake and release by a hydrogel intraocular lens and the human crystalline lens. *J. Cataract Refractive Surg.* **1989**, *15*, 169−175.
(16) Menon, I. A.; Trope, G. E.; Basu, P. K.; Wakeham, D. C.; Persad, S. D. Binding of timolol to iris-ciliary body and melanin: An in vitro model for assessing the kinetics and efficacy of long-acting antiglaucoma drugs. *J. Ocul. Pharmacol.* **1989**, *5*, 313−324.
(17) Ohtori, A.; Yamamoto, Y.; Tojo, K. J. Penetration and binding of aldose-reductase inhibitors in the lens. *Invest. Ophthalmol. Visual Sci.* **1991**, *32*, 189.
(18) Tang-Liu, D. D.-S.; Richman, J. B.; Liu, S. S. Lenticular uptake and distribution of xenobiotics and amino acids. *J. Ocul. Pharmacol. Ther.* **1992**, *8*, 267−277.
(19) Wang, L. Z.; Syn, N.; Li, S.; et al. The penetration and distribution of topical atropine in animal ocular tissues. *Acta Ophthalmol.* **2019**, *97*, No. e238.
(20) Mori, N.; Mochizuki, T.; Yamazaki, F.; et al. MALDI imaging mass spectrometry revealed atropine distribution in the ocular tissues and its transit from anterior to posterior regions in the whole-eye of rabbit after topical administration. *PLoS One* **2019**, *14*, No. e0211376.
(21) Nye-Wood, M. G.; Spraggins, J. M.; Caprioli, R. M.; Schey, K. L.; Donaldson, P. J.; Grey, A. C. Spatial distributions of glutathione and its endogenous conjugates in normal bovine lens and a model of lens aging. *Exp. Eye Res.* **2017**, *154*, 70−78.
(22) Ramsay, E.; Ruponen, M.; Picardat, T.; et al. Impact of chemical structure on conjunctival drug permeability: Adopting porcine conjunctiva and cassette dosing for construction of in silico model. *J. Pharm. Sci.* **2017**, *106*, 2463−2471.
(23) Kawamoto, T. Use of a new adhesive film for the preparation of multi-purpose fresh-frozen sections from hard tissues, whole-animals, insects and plants. *Arch. Histol. Cytol.* **2003**, *66*, 123−143.
(24) Vilupuru, A. S.; Glasser, A. Optical and biometric relationships of the isolated pig crystalline lens. *Ophthalmic Physiol. Opt.* **2001**, *21*, 296−311.
(25) Ranta, V.-P.; Laavola, M.; Toropainen, E.; Vellonen, K. S.; Talvitie, A.; Urtti, A. Ocular pharmacokinetic modeling using corneal absorption and desorption rates from in vitro permeation experiments with cultured corneal epithelial cells. *Pharm. Res.* **2003**, *20*, 1409−1416.
(26) Lee, V. H.; Luo, A. M.; Li, S. Y.; et al. Pharmacokinetic basis for nonadditivity of intraocular pressure lowering in timolol combinations. *Invest. Ophthalmol. Visual Sci.* **1991**, *32*, 2948.
(27) Guss, R.; Johnson, F.; Maurice, D. Rhodamine B as a test molecule in intraocular dynamics. *Invest. Ophthalmol. Visual Sci.* **1984**, *25*, 758−762.
(28) Kessel, D.; Beck, W. T.; Kukuruga, D.; Schulz, V. Characterization of multidrug resistance by fluorescent dyes. *Cancer Res* **1991**, *51*, 4665−4670.
(29) Oba, Y.; Poulson, S. R. Octanol-water partition coefficients (kow) vs. pH for fluorescent dye tracers (fluorescein, eosin Y), and implications for hydrologic tracer tests. *Geochem. J.* **2012**, *46*, 517−520.
(30) Urtti, A.; Salminen, L.; Periviita, L. Ocular distribution of topically applied adrenaline in albino and pigmented rabbits. *Acta Ophthalmol.* **2009**, *62*, 753−762.
(31) Sigurdsson, H. H.; Konráosdóttir, F.; Loftsson, T.; Stefánsson, E. Topical and systemic absorption in delivery of dexamethasone to the anterior and posterior segments of the eye. *Acta Ophthalmol. Scand.* **2007**, *85*, 598−602.
(32) del Amo, E. M.; Vellonen, K.-S.; Kidron, H.; Urtti, A. Intravitreal clearance and volume of distribution of compounds in rabbits: In silico prediction and pharmacokinetic simulations for drug development. *Eur. J. Pharm. Biopharm.* **2015**, *95*, 215−226.
(33) Ahmed, I.; Francoeur, M. L.; Thombre, A. G.; Patton, T. F. The kinetics of timolol in the rabbit lens: Implications for ocular drug delivery. *Pharm. Res.* **1989**, *06*, 772.
(34) Rzagalinski, I.; Volmer, D. A. Quantification of low molecular weight compounds by MALDI imaging mass spectrometry—A tutorial review. *Biochim. Biophys. Acta, Proteins Proteomics* **2017**, *1865*, 726−739.

DOI: 10.1021/acs.molpharmaceut.9b00585
Mol. Pharmaceutics 2019, 16, 3968−3976